Anal Bioanal Chem (2007) 389:2085–2095
DOI 10.1007/s00216-007-1555-x

REVIEW

Progress in direct solid sampling analysis using line source and high-resolution continuum source electrothermal atomic absorption spectrometry

Bernhard Welz · Maria Goreti R. Vale · Daniel L. G. Borges · Uwe Heitmann

Received: 4 July 2007 / Revised: 8 August 2007 / Accepted: 13 August 2007 / Published online: 5 September 2007

Abstract The literature about direct solid sample analysis of the past 10–15 years using electrothermal atomic absorption spectrometry has been reviewed. It was found that in the vast majority of publications aqueous standards were reported as having been used for calibration after careful program optimization. This means the frequently expressed claim that certified reference materials with a matrix composition and analyte content close to that of the sample have to be used for calibration in solid sample analysis is not confirmed in the more recent literature. There are obviously limitations, and there are examples in the literature where even calibration with certified reference materials did not lead to accurate results. In these cases the problem is typically associated with spectral interferences that cannot be corrected properly by the systems available for conventional line source atomic absorption spectrometry, including Zeeman-effect background correction. Using high-resolution continuum source atomic absorption spectrometry, spectral interferences become visible owing to the display of the spectral environment at both sides of the analytical line at high resolution, which makes program optimization straightforward. Any spectrally continuous background absorption is eliminated automatically, and even rapidly changing background absorption does not cause any artifacts, as measurement and correction of background absorption are truly simultaneous. Any kind of fine-structured background can be eliminated by "subtracting" reference spectra using a least-squares algorithm. Aqueous standards are used for calibration in all published applications of high-resolution continuum source atomic absorption spectrometry to direct solid sample analysis.

Keywords Direct solid sample analysis · Electrothermal atomic absorption spectrometry · High-resolution continuum source atomic absorption spectrometry · Background correction · Calibration

This contribution is based on a presentation given at the Colloquium for Analytical Atomic Spectroscopy (CANAS '07) held March 18–21, 2007 in Constance, Germany.

B. Welz (✉) · D. L. G. Borges
Departamento de Química,
Universidade Federal de Santa Catarina,
88040-900 Florianópolis, SC, Brazil
e-mail: w.bernardo@terra.com.br

B. Welz
Departamento de Química Analítica, Instituto de Química,
Universidade Federal da Bahia,
40170-290 Salvador, BA, Brazil

M. G. R. Vale
Instituto de Química, Universidade Federal do Rio Grande do Sul,
Av. Bento Gonçalves 9500,
91501-970 Porto Alegre, RS, Brazil

U. Heitmann
Department of Interface Spectroscopy,
ISAS—Institute for Analytical Sciences,
Albert-Einstein-Str. 9,
12489 Berlin, Germany

Introduction

Direct analysis of solid samples has been used since the early days of spectrochemical investigations, as might be exemplified by the investigations of Kirchhoff and Bunsen [1], who compared the black lines in the sun's spectrum with the absorption and emission spectra obtained with pure salts, introduced into the flame of a Bunsen burner using a little spoon. The experiments of Lockyer [2], using a coal-heated steel tube to measure absorption spectra of metals, which is shown in Fig. 1, and the famous King furnace [3]

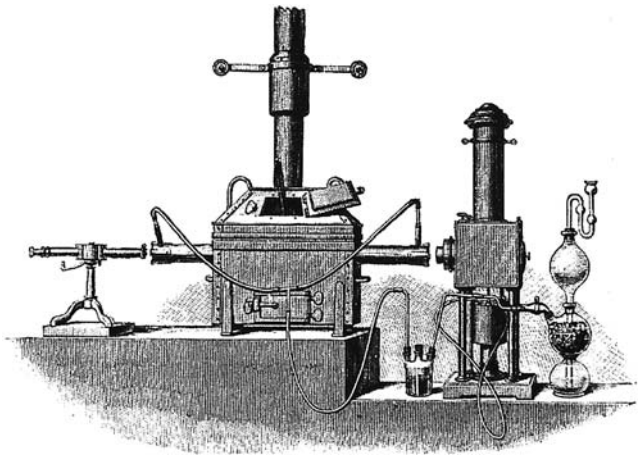

Fig. 1 Apparatus used by Lockyer [2] for atomic absorption measurements of metal vapors. Light source on the *right*; atomizer (iron tube mounted in a coal-fired furnace) in the *middle*, while hydrogen was generated in a Kipp's apparatus to provide a reducing atmosphere; spectroscope on the *left*

are just two more examples for the investigation of atomic absorption or emission spectra using solid samples. When spectrochemical analysis began to become popular during the first half of the twentieth century using arc and spark emission spectrometry, the analyses were typically carried out using solid samples. This practice is actually continuing today, for example, in metallurgical laboratories, where the majority of the analyses are still based on solid samples using these classic techniques and X-ray fluorescence spectrometry. Another technique that has been used extensively for direct analysis of solid samples is glow-discharge optical emission spectrometry [4].

In addition to these classic forms of direct solid sample (DSS) analysis, techniques such as laser ablation and electrothermal (ET) vaporization combined with inductively coupled plasma mass spectrometry have gained considerable interest over the past few decades, resulting in a significant number of publications [5, 6]. In most of these publications the advantages and limitations of DSS analysis have been clearly stated and/or became obvious from the results. Among the advantages are (1) the higher detection power, because direct solid sampling does not include any dilution, (2) higher speed of analysis, as usually only a minimum of sample preparation is necessary, (3) the risk of contamination and loss of the analyte element(s) is reduced to a minimum, as only very little sample handling is required, and (4) the use of toxic and/or corrosive chemicals is avoided. The major disadvantages, on the other hand, are (1) the natural inhomogeneity of most solid samples, which results in a higher relative standard deviation (RSD) of the results compared with solution analysis, typically between 10 and 20%, and (2) the need for certified reference materials (CRM) with an analyte content and a matrix composition as close to the sample investigated as possible for calibration. This latter practice is a kind of prerequirement in order to obtain accurate results in arc and spark emission as well as in X-ray fluorescence spectrometry analysis.

Direct solid sample analysis using electrothermal atomic absorption spectrometry

DSS analysis was actually the first application reported for ET atomic absorption spectrometry (AAS), back in 1957, when L'vov [7] put a "pinch of NaCl" into a graphite furnace that was standing unused in a corner of his laboratory, and watched how the radiation of a sodium lamp, passing through the furnace, disappeared upon heating the furnace. DSS analysis has been used ever since in ET AAS [8], as graphite furnaces allow a relatively easy introduction of solid samples, and the residence time of the sample vapor in the absorption volume is some 2–3 orders of magnitude longer than in a flame, making possible complete vaporization and atomization of even relatively large amounts of sample.

Several authors developed ET atomizers specifically for DSS analysis, such as Langmyhr [9] or Hadeishi and McLaughlin [10], while others developed tools for the convenient and reliable introduction of solid samples. There is also a relatively large number of specially designed graphite tubes, platforms, cups, etc. for DSS that have been offered commercially, and which are reviewed in detail in the book by Kurfürst [11].

In spite of these numerous, and at least in part successful attempts for DSS analysis with ET AAS, this approach was considered weird by the great majority of researchers in the field of atomic spectrometry. The major arguments against DSS ET AAS have been (1) the difficulty in handling and introducing the small sample mass reliably into the graphite tube atomizer, (2) the high imprecision of the results owing to the inhomogeneity of natural samples, which requires a large number of repetitive determinations, and (3) the difficulty in performing calibration, which usually required solid standards of composition and analyte content similar to those of the samples to be analyzed.

The first argument regarding the difficulty to handle and introduce a small sample mass into the graphite furnace was kind of approved in a review article about solid sampling in ET AAS by Bendicho and de Loos-Vollebregt [12]. These authors came to the conclusion that "the slurry technique gives better analytical performance than direct solid sampling." This judgment was largely based on the fact that "slurry introduction can be easily automated, hence combining the significant advantages of the solid and liquid sampling methods." This last quotation has ever since been

repeated in almost all publications about slurry sampling without considering that this statement was reflecting the situation in 1990. The above judgment was actually based on commercially available equipment [13], which consisted of a modified furnace autosampler, in which the slurries were homogenized by an ultrasonic probe immediately before their transfer to the graphite tube, whereas no comparably convenient tool was available for DSS at that time.

This situation has changed completely within the last decade. Firstly, because the abovementioned slurry autosampler has been withdrawn from the market and no comparable equipment is available nowadays. This means that all the well-known and well-described problems related to particle size distribution, specific gravity of the sample, and sedimentation errors [14–18] are back in slurry sampling. Secondly, there has been an ongoing effort to improve existing equipment for DSS analysis [19–22], which resulted in the introduction of a commercial device in the late 1990s, which included a pair of tweezers for the reproducible insertion of a graphite platform, containing the solid sample, into the graphite tube. Nowadays, the second generation of this solid sampling accessory is available both in a rugged and inexpensive manual version as well as in a fully automatic version, which is shown in Fig. 2. In the automatic version, the graphite platform with the solid sample is transferred first to an integrated microbalance, and then into the graphite tube, and the software automatically calculates the integrated absorbance normalized for a sample mass of 1 mg.

The second argument, i.e., the relatively high imprecision of the results due to the inhomogeneity of natural samples, is a well-known phenomenon in almost any kind of DSS analysis. It has been demonstrated that this problem is aggravated further owing to the small sample mass of around 1 mg that is typically introduced into the graphite furnace. However, the RSD of, e.g., five replicates in DSS ET AAS only rarely exceeds values of 10%, a value that is quite acceptable in many real situations, particularly in trace analysis. On the other hand, it has to be mentioned that DSS analysis offers the unique opportunity of carrying out homogeneity tests [23] and also of analyzing micro and submicro samples [11].

The third argument against DSS ET AAS, the need for solid CRM for calibration, was obviously transferred directly from arc and spark emission and X-ray fluorescence spectrometry. The need for solid CRM for calibration means in other words that there is a strong influence of the matrix on the analyte signal, i.e., interference. However, in ET AAS particularly nonspectral interference can be controlled to a great extent by the strict application of the stabilized temperature platform furnace (STPF) concept, introduced by Slavin et al. [24] in the early 1980s. The most important parts of this concept are atomization of the sample from a platform, the use of chemical modifiers to avoid analyte losses in the pyrolysis stage, and integration over the peak area in order to eliminate any influence of the matrix on the rate of analyte atomization. Later, the use of a transversely heated graphite tube was added in order to obtain a temporally and spatially homogeneous temperature distribution in the graphite tube during the atomization stage. Vale et al. [25] have shown in a recent review article that in the vast majority of articles published on DSS ET AAS during the last 10–15 years, aqueous standards were reported as having been used for calibration, i.e., interferences could be eliminated using careful program optimization. Table 1 gives an overview of the more recent publications on DSS ET AAS reporting use of conventional line source AAS and calibration against aqueous standards.

Fig. 2 Fully automatic accessory SSA 62 for automatic transfer of up to 62 SS platforms to a microbalance and into the graphite furnace. (Courtesy of Analytik Jena, Jena, Germany)

The limitations of conventional line source electrothermal atomic absorption spectrometry

Although conventional line source ET AAS with deuterium or Zeeman-effect background correction could apparently solve an impressive number of tasks with DSS, there are obvious limitations, and the present authors have given a good example for that in two publications about the determination of thallium in sediment samples. While the determination of thallium in river sediment could be carried out without any problem using DSS ET AAS and calibration against solid or aqueous standards and without a chemical modifier [45], the determination of the same analyte in marine sediments turned out to be impossible using the same conditions, and even using solid river sediment CRM for calibration [45]. Figure 3 shows the absorption signals for two of the sediment CRM analyzed

Table 1 Selected publications about direct solid sampling electrothermal (ET) atomic absorption spectrometry (AAS) using line source AAS and calibration against aqueous standards, covering the period 1995–2007

Matrix	Analyte	Background correction	Modifier	LOD	Remarks	Reference
Nickel-based alloys	Bi, Pb, Se, Te, Tl	Zeeman effect	Ni	NA	Single alloy chips	[26]
Molybdenum metal	Cu, K, Mg, Mn, Na, Zn	Deuterium	None	0.06–0.5 ng g^{-1}	Up to 80 mg sample introduced	[27]
Molybdenum silicide				0.5–4.5 ng g^{-1}		
High-purity tantalum powder	Cu, Fe, Mn, Na, Zn	Zeeman effect	None	0.1–27 ng g^{-1}	Up to 40 mg sample introduced	[19]
High-purity tantalum powder	Cu, Fe, K, Mn, Na, Zn	Deuterium	None	0.02–4 ng g^{-1}	Transversely heated atomizer	[20]
High-purity tungsten	Ca, Co, Cr, Cu, Fe, K, Mg, Mn, Na, Ni, Zn	Deuterium	None	0.01–4 ng g^{-1}	Up to 100 mg sample introduced	[28]
High-purity aluminum oxide	Co, Cr, Cu, Fe, K, Mg, Mn, Ni, Zn	Deuterium	None	0.25–25 ng g^{-1}		[29]
High-purity titanium	Al, As, Ca, Co, Cr, Cu, Fe, K, Mg, Mn, Na, Ni, Pb, Sn, Zn	Deuterium	Carbon powder	0.02–30 ng g^{-1}	Single pieces of metal; up to 30 mg sample introduced	[30]
High-purity tungsten trioxide and tungsten blue oxide	Ca, Co, Cr, Cu, Fe, K, Mg, Mn, Na, Ni, Zn	Deuterium	H_2 gas during pyrolysis	0.07–2 ng g^{-1} 0.01–1.7 ng g^{-1}	Up to 70 mg sample introduced	[31]
Niobium, titanium, and zirconium oxides	Si	Deuterium	CH_4 gas during pyrolysis	10 ng g^{-1}	3–15 mg sample introduced	[32]
Titanium dioxide	Fe, K, Mg, Mn, Na, Zn	Zeeman effect	None	0.06–0.7 ng g^{-1}	Two-step atomizer	[33]
Zirconium dioxide	Cd, Co, Cr, Cu, Fe, Li, Mn, Ni, Zn	Deuterium	None	0.06–2.3 ng g^{-1}	Graphite powder used for Cr determination	[34]
Soil, sulfide concentrate, and vitamin complex	Au	Deuterium	Pd	15 ng g^{-1}	Na_2CO_3 added to refractory samples	[35]
High-purity graphite and silicon carbide	Al, As, Ca, Cd, Co, Cr, Cu, Fe, K, Li, Mg, Na, Ni, Pb	Deuterium	None	0.1–50 ng g^{-1}	LODs better than with ETV-ICP OES, INAA, and slurry sampling	[36]
Crude oil	Ni, V	Deuterium	None/Pd	Ni, 20 ng g^{-1} V, 20 ng g^{-1}	Speciation analysis, volatile/nonvolatile species	[37]
Polymer, pharmaceutical drug, autocatalyst	Pd	Deuterium and Zeeman effect	None	0.4 ng g^{-1}	Gas flow during atomization; use of a secondary line	[38]
Plastic materials	P	Deuterium	Pd + ascorbic acid	2.5 μg g^{-1}		[39]
PVC	Sb	Deuterium	Pd	NA	Screening method	[40]
PVC	Sn	Deuterium	PO_4	NA		[41]
Polyamide	Si	Deuterium	Pt	100 ng g^{-1}		[42]
Polyethylene	Cr	NA	None	2 ng g^{-1}	LOD better than with ETV-ICP-MS	[43]
Barytes	Heavy metals	Deuterium	None	NA		[22]
Agricultural soil	Co, Zn	Deuterium	None	Co, 0.5 μg g^{-1} Zn, 4 μg g^{-1}	Gas flow during atomization 307.6-nm line for Zn	[44]
River sediments	Tl	Deuterium	None	20 ng g^{-1}		[45]
Marine sediments	Tl	Zeeman effect	Ru + NH_4NO_3	20 ng g^{-1}	Permanent modifier for solid sampling	[45]
Sediment	As	Deuterium	None	440 ng g^{-1}	Residues from leaching processes	[46]

Table 1 (continued)

Matrix	Analyte	Background correction	Modifier	LOD	Remarks	Reference
Environmental materials	Hg	Deuterium	Pd permanent	200 ng g^{-1}	$KMnO_4$ added to stabilize Hg in aqueous solutions	[47]
Sewage sludge	Cd	Deuterium	Pd	NA		[41]
Sewage sludge	Cr	NA	None	2 ng g^{-1}	LOD better than with ETV-ICP-MS	[43]
Sewage sludge	Cu, Pb	Deuterium	None	NA	Gas flow during atomization	[48]
Natural waters	Cr	Deuterium	None	20 ng L^{-1}	Coprecipitation with Pd/8-quinolinol/tannic acid	[49]
Seawater	As(III), As(V)	Deuterium	None	20 ng L^{-1}	Coprecipitation with Ni-PDC complex	[50]
Vitamin complex	Co, Zn	Deuterium	None	Co, 0.5 μg g^{-1} Zn, 4 μg g^{-1}	Gas flow during atomization 307.6-nm line for Zn	[44]
Vitamin–mineral tablets	Mn	Deuterium	None	NA	Comparison of calibration techniques	[51]
Biological samples	Cd, Cr, Mn, Pb	Deuterium	Pd (Cd only)	NA	Trace element distributions	[52]
Biological materials	Si	Deuterium	Pd + $Mg(NO_3)_2$	30 ng g^{-1}	Comparison with WDXRF and RNAA	[53]
Biological samples	Se	Zeeman effect	Pd + H_2SO_4 or Pd + HNO_3	3.3 ng g^{-1}	Preashing applied for preconcentration	[54]
Green coffee	Co, Mn	Deuterium	Pd +Mg + Triton X-100 (for Mn only)	Co, 4 ng g^{-1} Mn, 12 ng g^{-1}	403.1-nm line for Mn Comparison with ICP OES	[55]
Plant tissues	B	Deuterium	W (permanent) + citric acid + NH_4NO_3	300 ng g^{-1}	Two-step pyrolysis	[56]
Food samples	P	Deuterium	Pd + Ca	18 ng		[57]
Seafood	Hg, Cd, Mn, Pb, Sn	Zeeman-effect	None	0.0013–0.07 ng	Three-field Zeeman-effect background correction	[58]
Milk powder, lobster hepatopancreas	Cr	NA	None	2 ng g^{-1}	LOD better than with ETV-ICP-MS	[43]
Fresh meat	Cd, Pb	Deuterium	Pd + Mg + Triton X-100			[59]
Kidney, liver	Cd	Zeeman effect	None	NA	Wet animal tissue	[60]
Avian kidney	Pb, Cd, Hg	Zeeman effect	None	NA	Wet animal tissue	[61]
Bovine liver	Cu, Zn	Zeeman effect	Zn: W + Rh	Cu: 1.6 ng Zn: 1.3 ng	Cu: 216.5 nm Zn: 307.6 nm Microhomogeneity study	[62]
Several	Hg	Zeeman effect	None	8 ng g^{-1} (LOQ)	Ni–Cr tube with Pt platform; one-step program (900–1,000 °C)	[63]
Several	Ag	Zeeman effect and deuterium	Pd or HNO_3	2 ng g^{-1}	Distinct procedures for analysis of organic and inorganic samples	[64]

LOD limit of detection, *NA* not available, *ETV* electrothermal vaporization, *ICP* inductively coupled plasma, *OES* optical emission spectrometry, *INAA* instrumental neutron activation analysis, *MS* mass spectrometry, *PDC* pyrrolidine dithiocarbamate, *WDXRF* wavelength-dispersive X-ray fluorescence, *RNAA* radiochemical neutron activation analysis, *LOQ* limit of quantification

in this work using deuterium background correction, which obviously exhibit significant distortion owing to spectral interference. The results obtained under these conditions for a number of marine sediment CRM, using three different chemical modifiers, ammonium nitrate, a mixture of palladium and ammonium nitrates added in solution, and ruthenium as a permanent modifier plus ammonium nitrate added in solution, are shown in Table 2. There is no

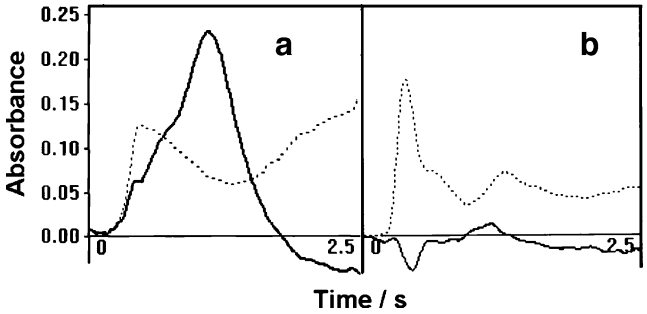

Fig. 3 Absorption signals for thallium (*solid line*) and background (*dotted line*) for marine sediment reference materials using reduced palladium as a chemical modifier and line source electrothermal atomic absorption spectrometry (ET AAS) with deuterium lamp background correction. **a** MESS-2 certified reference material (CRM); **b** HISS-1 CRM; 700 °C pyrolysis and 2,200 °C atomization temperature. (From [45])

agreement between the certified and the found values for most of the CRM, and there is little difference between the results obtained with the different modifiers.

In an attempt to find the source of the interference, the authors discovered a reasonably good correlation between the degree of signal suppression (with respect to the certified or recommended value) and the sulfur content of the CRM. This led to the assumption that a sulfur-containing diatomic molecule with rotational fine structure was responsible for the spectral interference. The obvious next step was to investigate Zeeman-effect background correction, which is known to be much better suited to correct for this kind of spectral interference. The signal shapes improved significantly compared with those shown in Fig. 3 [45], and the results obtained without a modifier, with ammonium nitrate, and with ruthenium as a permanent modifier and ammonium nitrate added in solution are shown in Table 3. It is obvious that without a modifier or with ammonium nitrate alone the results were still not satisfactory. Only with ruthenium applied as a permanent modifier, onto which the sediment was weighed, and the addition of ammonium nitrate solution to the sediment, it was possible to obtain results that did not differ from the certified or recommended values on a 95% confidence level.

Finally, high-resolution continuum source ET AAS (HR-CS ET AAS) was used to investigate the phenomenon, and the time- and wavelength-resolved absorption spectrum obtained under the conditions developed for conventional line source ET AAS is shown in Fig. 4 [65]. The absorption signal for thallium, which is barely visible in Fig. 4, is closely followed in time by a molecular absorption spectrum with pronounced fine structure and two atomic absorption lines of concomitant elements, the most pronounced one of which at 276.752 nm could be identified as a secondary iron line. Obviously, both the fine-structured molecular absorption and the atomic absorption due to matrix elements cause spectral interference with deuterium background correction, which is only capable of correcting for continuous background absorption. The atomic absorption due to iron should not cause any problems for Zeeman-effect background correction, as the line is far enough from

Table 2 Determination of thallium in marine certified reference materials (CRM) using direct solid sample (DSS) ET AAS with deuterium background correction and different chemical modifiers with calibration against NIST SRM 2704 (Buffalo River Sediment) as a solid standard

CRM	Certified value	Chemical modifier		
		NH_4NO_3	Pd + NH_4NO_3	Ru + NH_4NO_3
MESS-1[a]	0.7[c]	0.40±0.05	0.47±0.05	0.42±0.05
MESS-2[a]	0.98[c]	0.86±0.06	0.92±0.07	0.87±0.03
MESS-3[a]	0.9±0.06	0.83±0.05	0.92±0.10	0.85±0.10
PACS-2[a]	0.6[c]	0.11±0.07	0.20±0.10	0.21±0.06
BCSS-1[a]	0.6[c]	0.43±0.04	0.43±0.02	0.36±0.03
HISS-1[a]	0.06[c]	0.06±0.02	0.04±0.01	0.04±0.01
SRM 1646a[b]	<0.5[c]	0.16±0.02	0.14±0.02	0.10±0.02

[a] National Research Council Canada (NRCC), Ottawa, Canada
[b] National Institute of Standards and Technology (NIST), Gaithersburg, MD, USA
[c] Noncertified concentration
All values in micrograms per gram. (From [45])

Table 3 Determination of thallium in marine CRM using DSS ET AAS with Zeeman-effect background correction and different chemical modifiers. Calibration against aqueous standards using the same modifier

CRM	Certified value	Chemical modifier		
		Without	NH_4NO_3	Ru + NH_4NO_3
MESS-1[a]	0.7[c]	ND	ND	0.70±0.02
MESS-2[a]	0.98[c]	0.19± 0.01	0.72± 0.01	1.07±0.03
MESS-3[a]	0.9±0.06	ND	ND	1.08±0.07
PACS-2[a]	0.6[c]	0.12± 0.03	0.22± 0.04	0.58±0.02
BCSS-1[a]	0.6[c]	ND	ND	0.59±0.04
HISS-1[a]	0.06[c]	0.02± 0.002	0.03± 0.003	0.05±0.003
SRM 1646a[b]	<0.5[c]	ND	ND	0.20±0.02

ND not determined
[a] NRCC
[b] NIST
[c] Noncertified concentration
All values in micrograms per gram. (From [45])

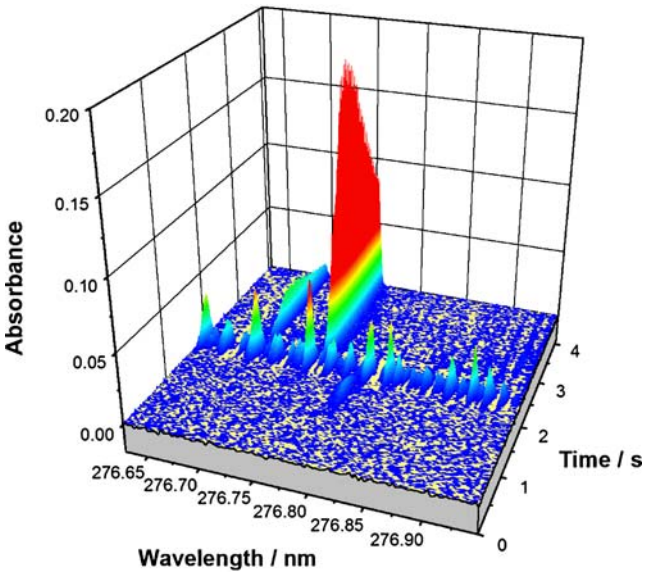

Fig. 4 Time- and wavelength-resolved absorption spectrum obtained for PACS-2 marine sediment CRM in the vicinity of the 276.787-nm thallium resonance line using high-resolution continuum source (HR-CS) ET AAS. Pyrolysis temperature 700 °C; atomization temperature 2,400 °C. (From [65])

the thallium line, even considering Zeeman splitting, to cause any line overlap. The forecast for the fine-structured molecular absorption is more difficult, as Zeeman-effect background correction can only correct for this kind of background if the molecular structure does not exhibit a Zeeman effect, i.e., if the background absorption without and with a magnetic field is exactly the same. An answer to this question can only be obtained from experiment.

Table 4 shows the results obtained for the same marine sediment CRM using HR-CS ET AAS and for essentially the same conditions as those that were used with Zeeman-effect background correction [65]. The only difference was that in this case slurry sampling had to be used, as the furnace used for these experiments did not allow DSS analysis, which however should not make any major difference. Surprisingly, the results were essentially the same without a modifier, with ammonium nitrate, and with the combination of ruthenium as a permanent modifier and the addition of ammonium nitrate, which means that no modifier is required when the determination is carried out by HR-CS ET AAS. As similar atomizers were used in conventional line source and in HR-CS ET AAS, differences observed in the two systems cannot be due to nonspectral interferences. Hence, the differences obtained without a modifier and with ammonium nitrate as a chemical modifier can only be due to spectral interference that does not affect the latter technique, most likely an alteration of the molecular spectrum in the presence of a magnetic field. It is not quite obvious why accurate results have been obtained with Zeeman-effect background correction with ruthenium as a permanent modifier, and the reason for that has not been further investigated.

High-resolution continuum source atomic absorption spectrometry

The previous example has already demonstrated the superior performance of HR-CS ET AAS, a technique that is fully described in the book by Welz et al. [66]. The purpose of this section is only to review briefly the special features of this system, which is based on the equipment described by Heitmann et al. [67]. It consists of a specially developed xenon short-arc lamp, operating in a hot-spot mode for maximum emission intensity in the far-UV range, a high-resolution double monochromator with a spectral bandwidth per pixel of 1.6 pm at 200 nm, and a charge coupled device array detector with full vertical binning. As only an intermediate and no exit slit is used, a segment of about 0.4 nm of the highly resolved spectrum reaches the detector, and is registered simultaneously by 200 pixels of the detector, all of which act as independent detectors. This way, the spectral environment of the analytical line becomes visible at high resolution, as shown in Fig. 4 for the example of thallium in marine sediment CRM.

As typically only three pixels are used to measure atomic absorption, all the other pixels can be used to correct for "spectrally continuous events," i.e., any alteration in the

Table 4 Determination of thallium in marine CRM using slurry sampling high-resolution continuum source (HR-CS) ET AAS and different chemical modifiers

CRM	Certified value	Chemical modifier		
		Without	NH_4NO_3	Ru + NH_4NO_3
MESS-1[a]	0.7[c]	0.57±0.01	0.53±0.01	0.58±0.01
MESS-2[a]	0.98[c]	0.98±0.02	1.02±0.01	0.99±0.02
MESS-3[a]	0.9± 0.06	0.93±0.04	1.03±0.01	1.02±0.015
PACS-2[a]	0.6[c]	0.50±0.01	0.55±0.01	0.52±0.005
BCSS-1[a]	0.6[c]	0.51±0.04	0.51±0.01	0.51±0.01
HISS-1[a]	0.06[c]	0.054± 0.01	0.057± 0.004	0.055±0.005
SRM 1646a[b]	<0.5[c]	0.20±0.02	0.18±0.01	0.17±0.01

[a] NRCC
[b] NIST
[c] Noncertified concentration
Calibration against aqueous standards using the same modifier. All values in micrograms per gram. (From [65])

radiation intensity that affects all pixels in the same way. This includes, for example, lamp flicker noise, but also any continuous background absorption, which is eliminated automatically. In addition, as illumination and readout of all pixels are strictly simultaneous, even the fastest changes in background absorption can be corrected without problem. After correction for spectrally continuous events, any spectrally discontinuous absorption, such as atomic absorption of the analyte and concomitants, as well as molecular absorption with rotational fine structure become visible, as can be seen in Fig. 4. Obviously, any concomitant atomic or molecular absorption that is not within the very small spectral window used to measure analyte absorption does not cause any spectral interference. ET AAS in addition offers the possibility to separate analyte and concomitant absorption in time by optimizing the temperature program. Last but not least, in situations where analyte and concomitant absorption cannot be separated, neither in time nor in wavelength, the system offers the possibility to measure and store a reference spectrum that can be subtracted from the sample spectrum using a least-squares algorithm [66]. In the case shown in Fig. 4, the fine-structured molecular spectrum could be removed completely by "atomizing" a solution of $KHSO_4$ and subtracting the recorded spectrum from the spectrum of the sediment CRM [65].

Direct solid sample analysis using high-resolution continuum source atomic absorption spectrometry

The articles published about DSS analysis using HR-CS ET AAS are compiled in Table 5. Quite some work has been invested in the analysis of mineral coal because of the enormous quantities of coal that are mined and burnt worldwide, and as this kind of sample is extremely difficult to be brought into solution. Using DSS, the only condition that had to be met was a pyrolysis temperature higher than 600 °C in order to avoid excessive continuous background absorption (up to absorbance $A=4$) due to radiation scattering at volatilized particles (soot, ash, etc.) [68, 70]. This problem was solved using a pyrolysis temperature of 700 °C, as shown in Fig. 5 for the example of thallium in coal, where the usually invisible uncorrected absorption over time is depicted in addition to the corrected signal, measured at the center pixel only. The uncorrected signal shows the residual continuous background absorption at the beginning of the atomization cycle as well as the lamp noise; both events are corrected perfectly, resulting in an absorption signal with extremely low noise. No modifier was required for the determination of thallium [68] and lead [70], whereas cadmium was lost in part at pyrolysis temperatures above 600 °C, hence necessitating a chemical modifier; iridium as a permanent modifier was found to be optimum to stabilize this analyte [69].

The analysis of biological materials might not be an ideal example for DSS, as they usually can be digested easily and rapidly. A motivation for using DSS might, however, be the increased detection power obtained with this technique if very low concentrations have to be determined. Another motivation might be the speed of analysis, as in the determination of toxic elements in fresh meat for screening purposes. However, this kind of application does not need HR-CS AAS, as has been shown in several publications using line source AAS [59, 61]. A third motivation could be an exceptionally high risk for systematic errors in the digestion step, and one of the analytes that is most affected by this risk is mercury.

Table 5 Publications about DSS analysis using HR-CS ET AAS with automatic correction for continuous background and calibration against aqueous standards

Matrix	Analyte	LOD	Remarks	Reference
Coal	Tl	10 ng g^{-1}	No modifier	[68]
Coal	Cd	2 ng g^{-1}	Ir permanent modifier	[69]
Coal	Pb	8 ng g^{-1}	No modifier	[70]
Biological materials	Co	5 ng g^{-1}	No modifier	[71]
Biological materials	Pb	10 ng g^{-1}	Ru permanent modifier	[72]
Biological materials	Hg	100 ng g^{-1}	No modifier, no pyrolysis stage; aqueous standards stabilized with $KMnO_4$	[73]

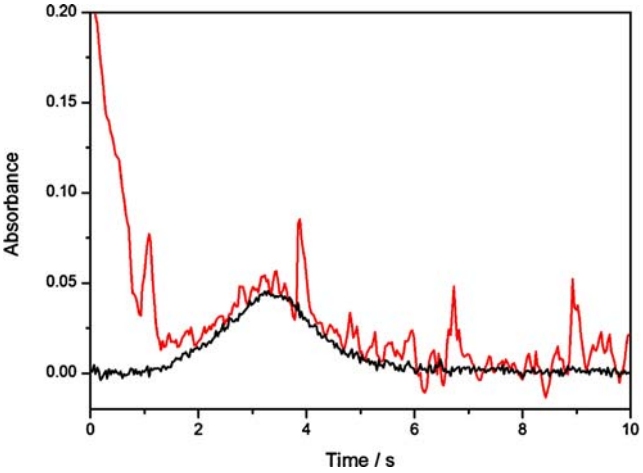

Fig. 5 Absorbance over time recorded for thallium in BCR 180 coal CRM at the 276.787-nm thallium resonance line using HR-CS ET AAS. Pyrolysis temperature 700 °C; atomization temperature 1,700 °C. *Red line* without background correction; *black line* with automatic correction for continuous background and lamp flicker noise

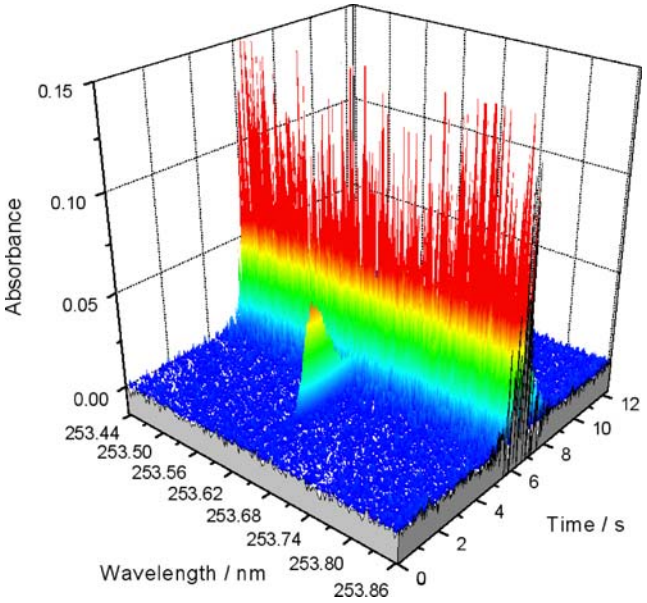

Fig. 6 Time- and wavelength-resolved absorption spectrum for DORM-1 Dogfish Muscle CRM (National Research council of Canada, Ottawa, Canada) in the environment of the analytical line for mercury at 253.652 nm using HR-CS ET AAS. Drying temperature 100 °C (3 s); atomization temperature 1,100 °C; no modifier used. (From [73])

The most sensitive technique for the determination of mercury is without any doubt the cold vapor technique coupled to AAS or atomic fluorescence spectrometry for detection. However, the cold vapor technique requires complete digestion of the organic matter and oxidation and stabilization of mercury as Hg^{2+}, usually using $KMnO_4$. Both the digestion and the stabilization include the risk of contamination, as even subboiling distillation cannot exclude mercury from the acids. In addition, for any surface with which mercury comes into contact there is the risk of exchange reactions, i.e., mercury might be adsorbed from samples with high analyte content and released to samples with low mercury content. All these problems are obviously minimized in the case of DSS analysis and, although the detection power of ET AAS is usually insufficient for the determination of mercury traces, DSS might compensate at least in part for the losses in sensitivity with this technique.

Silva et al. [73] investigated the determination of mercury in biological materials using DSS HR-CS ET AAS. The first problem they encountered was that the use of palladium as a permanent modifier, which proved to be successful in the determination of mercury in environmen-

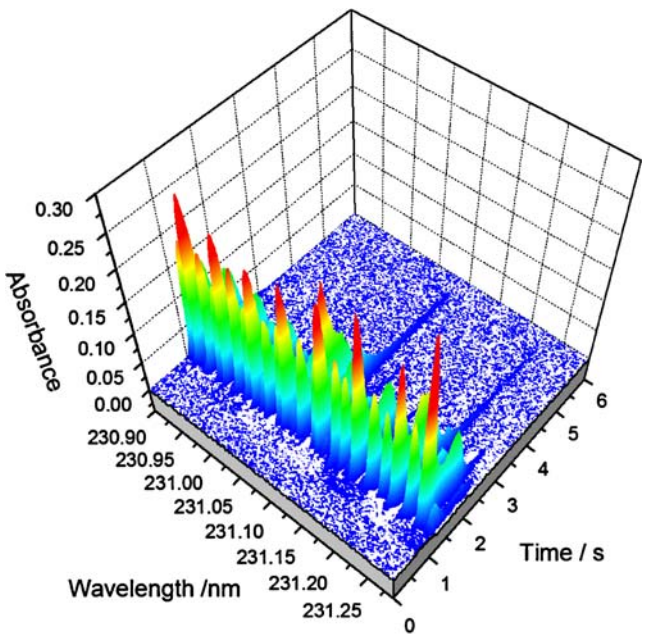

Fig. 7 Time- and wavelength-resolved absorption spectrum recorded for BCR 144R domestic sewage sludge in the vicinity of the 231.096-nm Ni line using HR-CS ET AAS. Pyrolysis temperature 1,100 °C; atomization temperature 2,500 °C. (From [75])

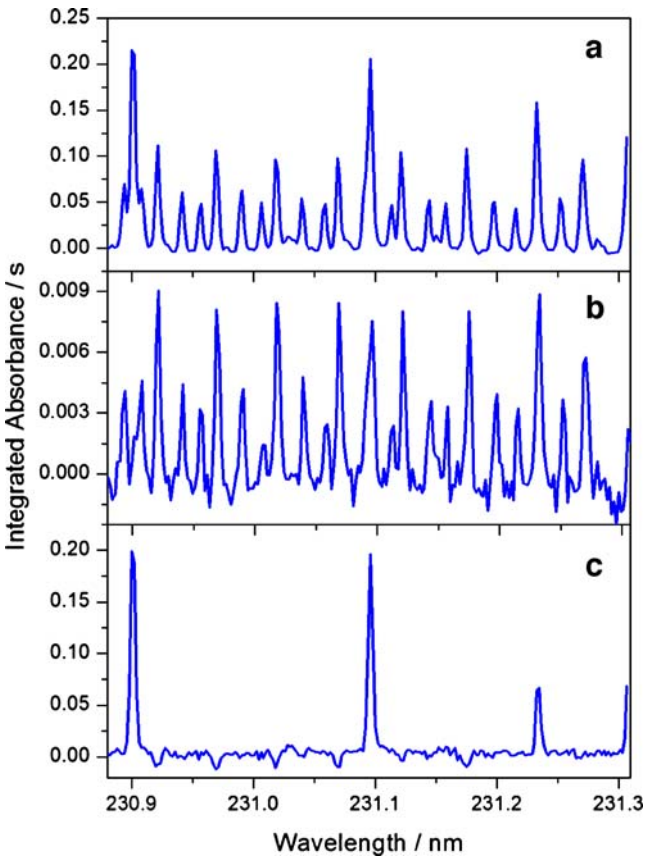

Fig. 8 Absorption spectra integrated over time in the vicinity of the secondary nickel line at 231.096 nm. Pyrolysis temperature 1,100 °C; atomization temperature 2,500 °C. **a** Spectrum for BCR 144R domestic sewage sludge; **b** reference spectrum of SiO, obtained from "atomization" of a 1,000 mg L^{-1} silicon standard solution; **c** sample spectrum after "subtraction" of the reference spectrum using least-squares background correction. (From [75])

tal samples [47], shifted the mercury absorption signal such that it appeared together with the excessive background absorption ($A \approx 4$) that was caused by the undigested organic matter. The second problem was that mercury in samples such as bovine muscle was reasonably stable up to about 250 °C, but was lost from fish samples already at temperatures above 100 °C. This was obviously due to the fact that mercury in fish predominantly occurs as methylmercury, which is much more volatile than inorganic mercury. The authors finally succeeded in adopting a temperature program without a pyrolysis stage and only 3 s of drying at 100 °C before they proceeded directly to the atomization stage at 1,100 °C. This way, it was possible to separate the analyte signal in time from the excessive baseline noise caused by radiation scattering that blocked off almost all the radiation from reaching the detector, as shown in Fig. 6. Such a situation cannot be handled by any of the background correction systems used in conventional line source AAS, as the sequential measurement of total and background absorption inevitably results in artifacts due to the rapidly changing background absorption, and hence in correction errors.

The determination of nickel in sewage sludge, which is still an ongoing research topic in our laboratory [75], appeared to be a particularly difficult case because of the large number of rotational lines that appeared within the spectral interval, as shown in Fig. 7. A less sensitive nickel line was chosen in this case in order to allow the introduction of a reasonably large sample volume into the graphite tube. However, the solution proved to be easier than expected, as the molecular absorption spectrum was found to be due to a single molecule, SiO, which could be created without problems by "atomizing" a 1,000 mg L^{-1} silicon standard solution, as shown in Fig. 8. After subtraction of the reference spectrum from the sample spectrum using a least-squares algorithm, which is part of the software, only three atomic lines remain visible, two nickel lines at 231.096 and 231.234 nm and one cobalt line at 230.901 nm that is directly overlapped by an iron line at 230.900 nm.

While this analytical task could be solved without difficulties using HR-CS ET AAS, it would for sure have been more complex for classic line source AAS. Neither deuterium nor Smith–Hieftje background correction [74] would be capable of handling this kind of fine-structured molecular absorption; the former technique averages the background over the part of the spectrum that passes the exit slit, whereas the latter one measures the background at both sides of the analytical line. In both cases the background subtracted from the total absorbance measured at the analytical line would be different from the actual background at this wavelength, because a molecular "line" is overlapping with the nickel line, as can easily be seen in the spectra in Fig. 8. It is not possible to predict to which extent Zeeman-effect background correction could handle this kind of fine-structured molecular absorption, as it is unknown if the spectrum of SiO is affected by the magnetic field. However, because of the direct overlap of a molecular absorption line with the atomic absorption line for nickel, any minor change of the molecular absorption due to the magnetic field would inevitably result in a correction error.

Conclusion

It was surprising to realize that in the vast majority of publications about DSS analysis with ET AAS over the past 10–15 years aqueous standards were reported to have been used for calibration even in the presence of very complex matrices. This means that any kind of matrix influence could be eliminated in these cases, so there was no need to use solid CRM for calibration, a requirement that has often been claimed in the literature. Obviously, careful method development was usually a prerequisite for success, and this stage has often been quite tedious. However, there are also some publications that appear to be the exception to this "rule," and there are cases where even calibration against solid CRM did not bring the expected result. At least in some of these cases it could be clearly shown that the difficulties were due to spectral interferences that could not be handled by the background correction systems available for line source AAS. In contrast, all the tasks regarding DSS analysis investigated up to now by HR-CS ET AAS could be solved without problems using aqueous standards for calibration owing to the far superior background correction capabilities of this technique. In addition, method development is greatly facilitated owing to the visibility of the spectral environment around the analytical line at high resolution. The possibility to optimize analytical conditions after a determination (postprocessing) without the need for a new determination reduces further the time required for method development. In essence, HR-CS ET AAS makes DSS analysis a very attractive alternative to solution analysis, at least for samples that are difficult to be brought into solution and/or which are particularly affected by contamination problems.

Acknowledgements The authors are grateful to Conselho Nacional de Desenvolvimento Científico e Tecnológico (CNPq) and to Fundação de Amparo à Pesquisa do Estado da Bahia (FAPESB) for financial support. M.G.R.V. and D.L.G.B. have scholarships from CNPq and B.W. has a research scholarship from FAPESB. Moreover, financial support from the Senatsverwaltung für Wissenschaft, Forschung und Kultur des Landes Berlin, the Deutsche Forschungsgemeinschaft, and the Bundesministerium für Bildung und Forschung is gratefully acknowledged.

References

1. Kirchhoff G, Bunsen R (1860) Philos Mag 20:89
2. Lockyer JN (1878) Studies in spectrum analysis. Appleton, London
3. King AS (1908) Astrophys J 28:300
4. Grimm W (1968) Spectrochim Acta Part B 23:443
5. Beauchemin D, Grégoire DC, Günter D, Karanassios V, Mermet JM, Wood TJ (eds) (2000) Discrete sample introduction techniques for inductively coupled plasma mass spectrometry. Comprehensive analytical chemistry, vol XXXIV. Elsevier, Amsterdam
6. Becker JS (2007) Inorganic mass spectrometry. Wiley, New York
7. L'vov, BV (1984) Spectrochim Acta Part B 39:149
8. Welz B, Sperling M (1999) Atomic absorption spectrometry, 3rd edn. Wiley-VCH, Weinheim, pp 56–61
9. Langmyhr FJ (1977) Talanta 24:277
10. Hadeishi T, McLaughlin R (1985) Fresenius Z Anal Chem 322:657
11. Kurfürst U (1998) Solid sample analysis. Springer, Berlin Heidelberg New York
12. Bendicho C, de Loos-Vollebregt MTC (1991) J Anal At Spectrom 6:353
13. Carnrick GR, Daley G, Fotinopoulos A (1989) At Spectrosc 10:170
14. Miller-Ihli NJ (1997) J Anal At Spectrom 12:205
15. Majidi VJ, Holcombe JA (1990) Spectrochim Acta Part B 45:753
16. Miller-Ihli NJ (1997) Spectrochim Acta Part B 52:431
17. Silva MM, Vale MGR, Caramão EB (1999) Talanta 50:1035
18. Laborda F, Górriz MP, Castillo JR (2004) Talanta 64:631
19. Friese KC, Krivan V, Schuierer O (1996) Spectrochim Acta Part B 51:1223
20. Friese KC, Krivan V (1998) Spectrochim Acta Part B 53:1069
21. Nowka R, Müller H (1997) Fresenius J Anal Chem 359:132
22. Nowka R, Marr IL, Ansari TM, Müller H (1999) Fresenius J Anal Chem 364:533
23. Ihnat M, Stoeppler M (1990) Fresenius J Anal Chem 338:455
24. Slavin W, Manning DC, Carnrick GR (1981) At Spectrosc 2:137
25. Vale MGR, Oleszczuk N, dos Santos WNL (2006) Appl Spectrosc Rev 41:377
26. Irwin R, Mikkelsen A, Michel RG, Daugherty JP, Preli FR (1990) Spectrochim Acta Part B 45:903
27. Dočekal B, Krivan V (1995) Spectrochim Acta Part B 50:517
28. Hornung M, Krivan V (1998) Anal Chem 70:3444
29. Lucic M, Krivan V (1998) J Anal At Spectrom 13:1133
30. Krivan V, Huang MD (1998) Anal Chem 70:5312
31. Hornung M, Krivan V (1999) Spectrochim Acta Part B 54:1177
32. Huang MD, Krivan V (2001) Spectrochim Acta Part B 56:1645
33. Friese KC, Huang MD, Schlemmer G, Krivan V (2006) Spectrochim Acta Part B 61:1054
34. Krivan V, Janickova P (2005) Anal Bioanal Chem 382:1949
35. Resano M, Aramendia M, Garcia-Ruiz E, Belarra MA (2005) J Anal Atom Spectrom 20:479
36. Schaeffer U, Krivan V (2001) Fresenius J Anal Chem 371:859
37. Silva MM, Damin, ICF, Vale MGR, Welz B (2007) Talanta 71:1877
38. Resano M, Garcia-Ruiz E, Crespo C, Vanhaecke F, Belarra MA (2003) J Anal At Spectrom 18:1477
39. Resano M, Belarra MA, Castillo JR, Vanhaecke F (2000) J Anal At Spectrom 15:1383
40. Belarra MA, Belategui I, Lavilla I, Anzano JM, Castillo JR (1998) Talanta 46:1265
41. Belarra MA, Resano M, Rodríguez S, Urchaga J, Castillo JR (1999) Spectrochim Acta Part B 54:787
42. Resano M, Aramendía M, Volynsky AB, Belarra MA (2004) Spectrochim Acta Part B 59:523
43. Resano M, Garcia-Ruiz E, Vanhaecke F, Crespo C, Belarra MA (2004) J Anal At Spectrom 19:958
44. Belarra MA, Crespo C, Martinez-Garbayo MP, Resano M (2003) Spectrochim Acta Part B 58:1847
45. Vale MGR, Silva MM, Welz B, Nowka R (2002) J Anal At Spectrom 17:38
46. Sauquillo A, Rauret G, Rehnert A, Muntau H (2003) Anal Chim Acta 476:15
47. Silva AF, Welz B, Curtius AJ (2002) Spectrochim Acta Part B 57:2031
48. Belarra MA, Crespo C, Resano M, Castillo JR (2000) Spectrochim Acta Part B 55:865
49. Zhang QB, Minami H, Inoue S, Atsuya I (1999) Anal Chim Acta 401:277
50. Zhang QB, Minami H, Inoue S, Atsuya I (2004) Anal Chim Acta 508:99
51. Coşkun N, Akman S (2004) Talanta 64:496
52. Štupar J, Dolinšek F (1996) Spectrochim Acta Part B 51:665
53. Huang MD, Krivan V (2007) Spectrochim Acta Part B 62:297
54. Minami H, Inoue Y, Sakata K, Atsuya I (1997) Anal Sci 13:397
55. Oleszczuk N, Castro JT, Silva MM, Korn MGA, Welz B, Vale MGR (2007) DOI 10.1016/j.talanta.2007.05.005
56. Resano M, Briceno J, Aramendia M, Belarra MA (2007) Anal Chim Acta 582:14
57. Coşkun N, Akman S (2005) Spectrochim Acta Part B 60:415
58. Detcheva A, Grobecker KH (2006) Spectrochim Acta Part B 61:454
59. Damin ICF, Silva MM, Vale MGR, Welz B (2007) DOI 10.1016/j.sab.2007.05.007
60. Lücker E, Schuierer O (1996) Spectrochim Acta Part B 51:201
61. Lücker E (1997) Fresenius J Anal Chem 358:848
62. Nomura CS, Silva CS, Nogueira ARA, Oliveira PV (2005) Spectrochim Acta Part B 60:673
63. Grobecker KH, Detcheva A (2006) Talanta 70:962
64. Resano M, Aramendia M, Garcia-Ruiz E, Crespo C, Belarra MA (2006) Anal Chim Acta 571:142
65. Welz B, Vale MGR, Silva MM, Becker-Ross H, Huang MD, Florek S, Heitmann U (2002) Spectrochim Acta Part B 57:1043
66. Welz B, Becker-Ross H, Florek S, Heitmann U (2005) High-resolution continuum source AAS—the better way to do atomic absorption spectrometry. Wiley-VCH, Weinheim
67. Heitmann U, Schütz M, Becker-Ross H, Florek S (1996) Spectrochim Acta Part B 51:1095
68. Silva AF, Borges DLG, Welz B, Vale MGR, Silva MM, Klassen A, Heitmann U (2004) Spectrochim Acta Part B 59:841
69. Silva AF, Borges DLG, Lepri FG, Welz B, Curtius AJ, Heitmann U (2005) Anal Bioanal Chem 382:1835
70. Borges DLG, Silva AF, Curtius AJ, Welz B, Heitmann U (2006) Microchim Acta 154:101
71. Ribeiro AS, Vieira MA, Silva AF, Borges DLG, Welz B, Heitmann U, Curtius AJ (2005) Spectrochim Acta Part B 60:693
72. Borges DLG, Silva AF, Welz B, Curtius AJ, Heitmann U (2006) J Anal At Spectrom 21:763
73. Silva AF, Lepri FG, Borges DLG, Welz B, Curtius AJ, Heitmann U (2006) J Anal At Spectrom 21:1321
74. Smith SB, Hieftje GM (1983) Appl Spectrosc 37:419
75. Pedroso ML, Borges DLG, Bascuñan VLAF, Welz B, Heitmann U (2006) In: 9th Rio symposium on atomic spectrometry, book of abstracts, 196